

Thermal behavior of metallic aluminum in a container glass melt

Renate Reisch, Dörte Stachel, Steffi Traufelder and Elke Tessmann

Otto-Schott-Institut für Glaschemie, Friedrich-Schiller-Universität, Jena (Germany)

The thermal behavior of metallic aluminum was studied in the temperature range of 1100 to 1500 °C in a container glass melt. The dissolution of the metal was determined as a function of aluminum input, glass volume, melting time and the type of glass used. By analogy, melts containing magnesium cuttings were also investigated.

With the aid of electron microscopy, it was possible to establish a reaction scheme of oxidation and reduction processes. Only 2 to 3% of the aluminum introduced causes the formation of silicon spheres. The main part will be oxidized through reactions with oxygen, hydroxide and polyvalent ions in the melt.

Thermisches Verhalten von Aluminium in einer Behälterglasschmelze

Das thermische Verhalten von Aluminiumspänen wurde in einer Behälterglasschmelze im Temperaturbereich von 1100 bis 1500 °C untersucht. Die Auflösung des Metalls wurde in Abhängigkeit von der eingebrachten Aluminiummenge, dem Glasvolumen, der Schmelzzeit und dem Glastype bestimmt. Zum Vergleich wurden Schmelzen mit Magnesiumspänen durchgeführt.

Mit Hilfe der Elektronenmikroskopie war es möglich, ein Reaktionsschema für die ablaufenden Vorgänge in der Glasschmelze aufzustellen. Nur 2 bis 3% des eingesetzten Aluminiums verursachen die Bildung von Siliciumkugeln. Der Hauptteil des Aluminiums wird durch Wechselwirkung mit dem in der Schmelze gelösten Sauerstoff, den Hydroxid- und polyvalenten Ionen oxidiert.

1. Introduction

Up to now, reactions between metallic impurities and glass melts have been examined scarcely because in the past resulting problems were not serious. With improvement of melting tanks, installation of electric boosting and bubbling, the temperatures at the bottom were increased. If metals are present in the melt, bottom corrosion is observed at higher temperatures [1].

Further problems appeared through increased use of recycled cullet because metallic contaminations cannot be completely avoided. Metallic aluminum entering the furnace as foil, aluminized paper, caps and rings leads to the formation of spheres of elementary silicon possessing a mean size of 1 mm. These inclusions cause stresses in the glass and the container must be rejected [2 to 4]. To reduce production losses, information on reactions occurring between metal and glass melt is necessary. This paper reports on the reaction behavior of aluminum and magnesium cuttings in a container glass melt and the silicon spheres formed.

2. Oxidation and reaction behavior of aluminum

The oxidation of aluminum is a complicated process which e. g. depends on occurring impurities and coatings.

During the oxidation process at high temperatures, first an amorphous phase is formed. After long annealing time crystalline Al_2O_3 , α - and γ -phase, is observed [5 and 6]. The oxide layer grows due to diffusion of aluminum ions through this layer. On the surface the aluminum rapidly reacts with oxygen and hence, new alumina is formed. The diffusion process is caused by a diffusion via lattice defects in the oxide layer. The formed thin oxide layer passivates the surface and the further growth of the layer will be diffusion-controlled and hence, follows a square root law. If the oxide layer, however, is removed or scratched, the oxidation is enhanced. Alloying elements such as magnesium, iron, silicon, copper, zinc, manganese, calcium and beryllium accelerate the oxidation process [7]. The oxide layers are gray-colored because metallic inclusions are still present [8]. The layer will be white, if all metallic particles are completely oxidized. As shown in the phase diagram [9] (figure 1), small additions of silicon decrease the melting temperature of aluminum. The alloy with the eutectic composition has good processing properties and is technologically important. After cooling the silicon is embedded in the aluminum matrix phase in different crystalline forms [6].

On the basis of the Ellingham diagram [10], aluminum reduces many oxides such as SiO_2 , Fe_2O_3 , MnO , TiO_2 , SnO_2 , ZnO , Cu_2O and Cr_2O_3 . Not only SiO_2 but

Received February 21, 1996.

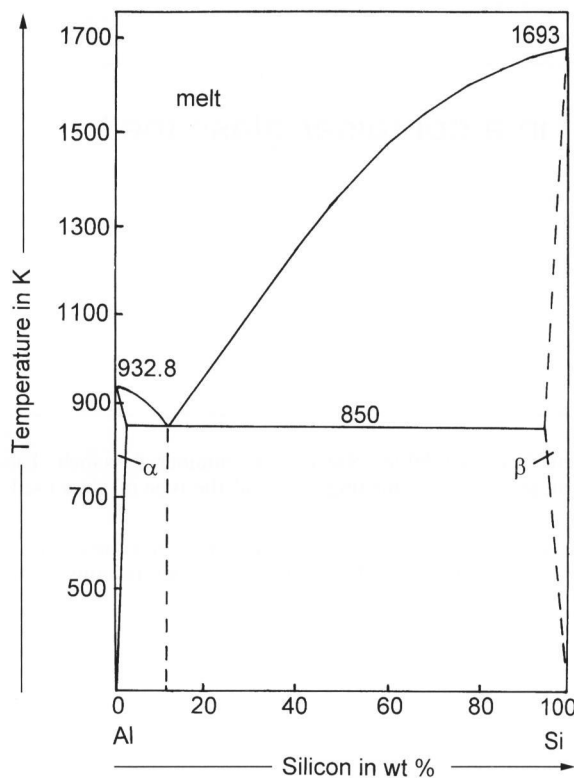


Figure 1. Phase diagram of the system aluminum–silicon [9].

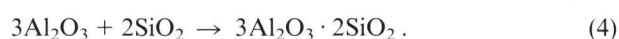
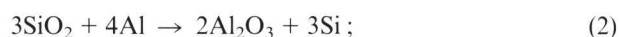
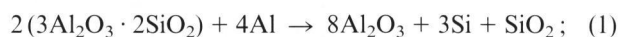
Table 1. Quantity of formed silicon spheres and color of glass as a function of aluminum input

aluminum input in g	quantity of silicon spheres	color of glass
batch without refining agent		
0.01	0	greenish
0.02	3	greenish with brown cords
0.03	n. d.	brown-black regions with bubbles
batch with refining agent		
0.01	0	greenish with brown cords
0.02	0	green with brown cords
0.03	7	greenish

Explanations: n. d. = The spheres could not be determined quantitatively due to the strong black-colored glass.

Experimental conditions: melted from raw materials, 118 g batch. Melting conditions: heating up to 1550 °C and annealing 4 h at 1550 °C, cooling starts in a furnace at 560 °C.

also mullite will be reduced and metallic silicon is formed according to [4, equation (1)],



Reaction (2) takes place at temperatures above 700 °C. Studies of mixtures of quartz sand and aluminum showed that the reaction mechanism is more complicated and also aluminum–silicon alloys and mullite can be formed. The formation of mullite was solely observed at higher temperatures. Reaction (4) will be accelerated, however, by the quartz–cristobalite phase transformation.

Shardakov [11] examined the reactions between an Al–Fe alloy and a glass melt. He also observed silicon, Al_2O_3 , mullite and as additional phase Fe_2O_3 . Standage and Gani [12] showed that the occurrence of bismuth and antimony as alloying metals leads to the formation of an oxide layer on the surface, which accelerates the reduction of SiO_2 by molten aluminum.

The studies by Weiser, Petermüller, Wohlleben, Schumacher, Wischnat and Roger [2 to 4 and 13 to 15] confirmed that metallic aluminum impurities cause the formation of silicon spheres in the container glass melt. But an exact reaction mechanism was not given.

3. Container glass melts with aluminum cuttings

The experiments were carried out on a flint glass. In industrial practice, it was observed that with this glass type more silicon spheres appear than in green and amber glass. Moreover, the possibilities to observe the aluminum dissolution and the formation of silicon spheres in flint glass are better than in colored container glass.

Either batch or cullet was used as raw material and melted in alumina crucibles. The batch consisted of a three-component system with the composition (in mol%): 12.25 Na_2O , 11.40 CaO and 76.35 SiO_2 . Raw materials used were: sodium carbonate, calcium carbonate and quartz sand from Oberland Glas AG, Bad Wurzach (Germany). As refining agent sodium sulfate was added (0.25 g/100 g glass) as well as cuttings of metallic aluminum. The cullet had a grain size of less than 3.15 mm and was also obtained from Oberland Glas. Subsequent to the melting process, the glass melt was annealed at 1550 °C for 4 h.

As shown in table 1, already small quantities of aluminum cause the formation of silicon inclusions. Further experiments were carried out, refining agents being added and the melting conditions varied (see tables 1 to 3). They showed that the dissolution of aluminum metal depends on oxygen partial pressure in glass melt as well as on melting temperature, melting time, the amount of aluminum and the glass volume. An influence of the amount of cullet was not found. The dissolution rate of aluminum in a 100 g container glass melt is so low that long melting times (32 h) at high melting temperatures are necessary to obtain clear glass melts (table 2). By contrast, after melting at temperatures in the range of 1100 to 1300 °C, gray, brown and black-colored glass melts are observed. There, the color intensity increases with annealing time and the quantity of

Table 2. Long-time annealing experiments of flint glass melts

temperature in °C	annealing time in h		
	4	16	32
1200	gray regions at the surface	gray-brown regions with silicon spheres	dark brown-gray regions with inclusions
1300	gray-brown regions with metallic spheres	dark brown-gray regions with silicon	dark brown-gray regions with spheres
1400	gray-brown regions with metallic spheres	brown, black regions	light brown regions with small spheres
1500	gray-black regions	clear glass with metallic spheres	clear glass

Experimental conditions: 50 g cullet, grain size between 1.25 and 3.15 mm, 0.1 g aluminum, cuttings in the middle of the crucible.

aluminum added. However, at temperatures above 1300 °C, the color intensity decreases with annealing time because formed Al_2O_3 will be dissolved in the glass melt. Also the formed silicon spheres dissolve but, by comparison, more slowly. With increasing volume of the melt, the dissolution time becomes shorter with a constant quantity of aluminum added (table 3).

The gray and black glass regions were examined using a scanning electron microscope (SEM). The SEM micrographs (see section 5.) showed that different phases occur in these regions. If the aluminum input is low, the colored glass regions are found at the surface and at high aluminum inputs on the bottom of the crucible. When long annealing times of more than 16 h are used, the silicon spheres and the aluminum-rich glass can cause crucible corrosion.

In table 4 the densities of metals, their oxides and container glass are summarized. Silicon and liquid aluminum must rise to the surface of the glass melt, due to their lower density. The Al_2O_3 and mullite formed must deposit at the bottom of the crucible, due to their higher density. The alumina formed increases the viscosity of the container glass melt during its dissolution and hence, diffusion processes are decelerated. Concentration gradients in the melt as well as differences in surface tension cause microturbulences (Marangoni effect) in the gray glass regions.

After Bauermeister [18] dissolution of Al_2O_3 only takes place with low reaction rate and by forming of bubbles. These results were also observed if metallic aluminum was added.

To clarify the dependence on glass melt composition, further studies using green and amber cullet were carried out. The input of aluminum was 0.1 g. The cullet was melted at different temperatures as shown in table 5. At low temperatures also black-colored glass regions occur. The observed differences to flint glass were: the decreased number of silicon spheres formed, the occurrence of white, bubble-rich inclusions and, in the case of amber glass, the presence of silicon spheres surrounded by a gray-brownish glass phase.

Table 3. Dissolution of aluminum at higher melting volume

aluminum input in g	annealing conditions		observations
	tempera- ture in °C	time in h	
0.1	1300	48	brown glass with small gray regions and silicon spheres at the surface
0.1	1400	30	yellow-greenish glass with brown cords, at the surface only one small gray region
0.1	1500	10	yellow-greenish glass

Experimental conditions: 100 g flint glass cullet, grain size below 1.25 mm, cuttings put in the middle of the crucible.

Table 4. Density and expansion coefficients of metals, their oxides and container glass [16 and 17]

compound	density in g/cm^3	thermal expansion coefficient in 10^{-6}K^{-1}
Al (solid)	2.70	23.80
Al (liquid)	2.38	7.00
Si	2.33	2.50
$\alpha\text{-Al}_2\text{O}_3$	3.95	7.00
$\beta\text{-Al}_2\text{O}_3$	3.30	4.00
$\gamma\text{-Al}_2\text{O}_3$	3.47	—
$\beta\text{-quartz}$	2.65	12.30
$\alpha\text{-quartz}$	2.60	—
$\alpha\text{-tridymite}$	2.30	—
$\alpha\text{-cristobalite}$	2.21	—
container glass	2.48	9.00
$3\text{Al}_2\text{O}_3 \cdot 2\text{SiO}_2$	3.16	4.50
$\text{Al}_2\text{O}_3 \cdot \text{SiO}_2$	3.25	3.20

4. Glass melts with magnesium cuttings

Magnesium is a stronger reduction agent than aluminum. After Schumacher and Petermüller [3 and 13] this metal does not cause the formation of silicon spheres in

Table 5. Effect of glass melt composition on dissolution of aluminum (0.1 g aluminum per 100 g cullet)

melting conditions		flint glass	green glass	amber glass
temperature in °C	time in h			
1100	3	gray glass at the surface, brown cords	gray glass at the surface	gray glass at the surface
1200	3	gray glass at the surface, brown cords	gray glass at the surface	gray glass at the surface
1300	3	8 silicon spheres at the surface, brown cords	3 silicon spheres at the surface, white inclusions with many bubbles	3 silicon spheres at the surface, white inclusions with many bubbles
1500	3	6 silicon spheres at the surface	1 silicon sphere at the surface	1 silicon sphere at the surface

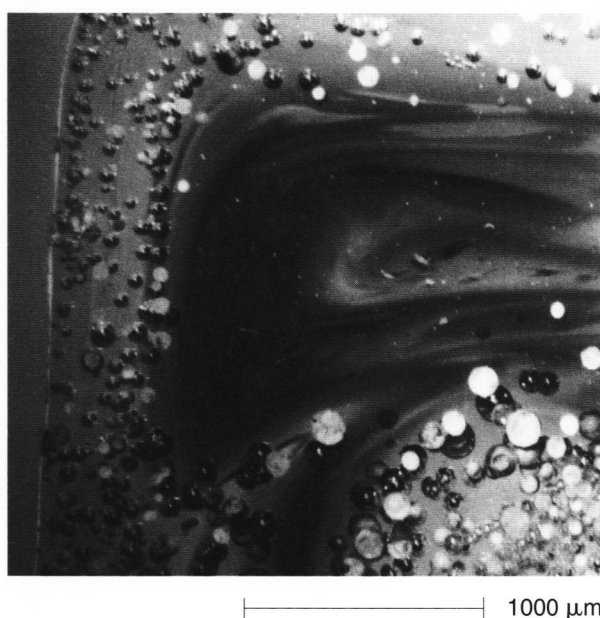


Figure 2. SEM micrograph of formed black cords and bubbles at high magnesium additions to a container glass melt (melt with 3.4 g Mg to 100 g cullet, melted at 1550 °C for 1 h).

a green container glass melt. To reexamine this result, a series of melts with raw materials was carried out. The batches were melted for 1 or 4 h at 1550 °C.

Small quantities of magnesium were dissolved and silicon spheres did not appear. With increasing input of magnesium, blue, yellow and brown colorations were observed in the flint glass. Silicon spheres were first observed at inputs of 1 g magnesium to 50 g glass. Longer melting times were necessary to obtain clear glass without cords and bubbles. Figure 2 shows the obtained black cords and bubbles after a melting time of 1 h. At lower melting temperatures (1100 and 1200 °C) also gray regions at the surface of the melt were observed and examined using SEM.

5. Scanning electron microscopy

The silicon spheres obtained and the gray glass regions formed were separated from the glass and examined

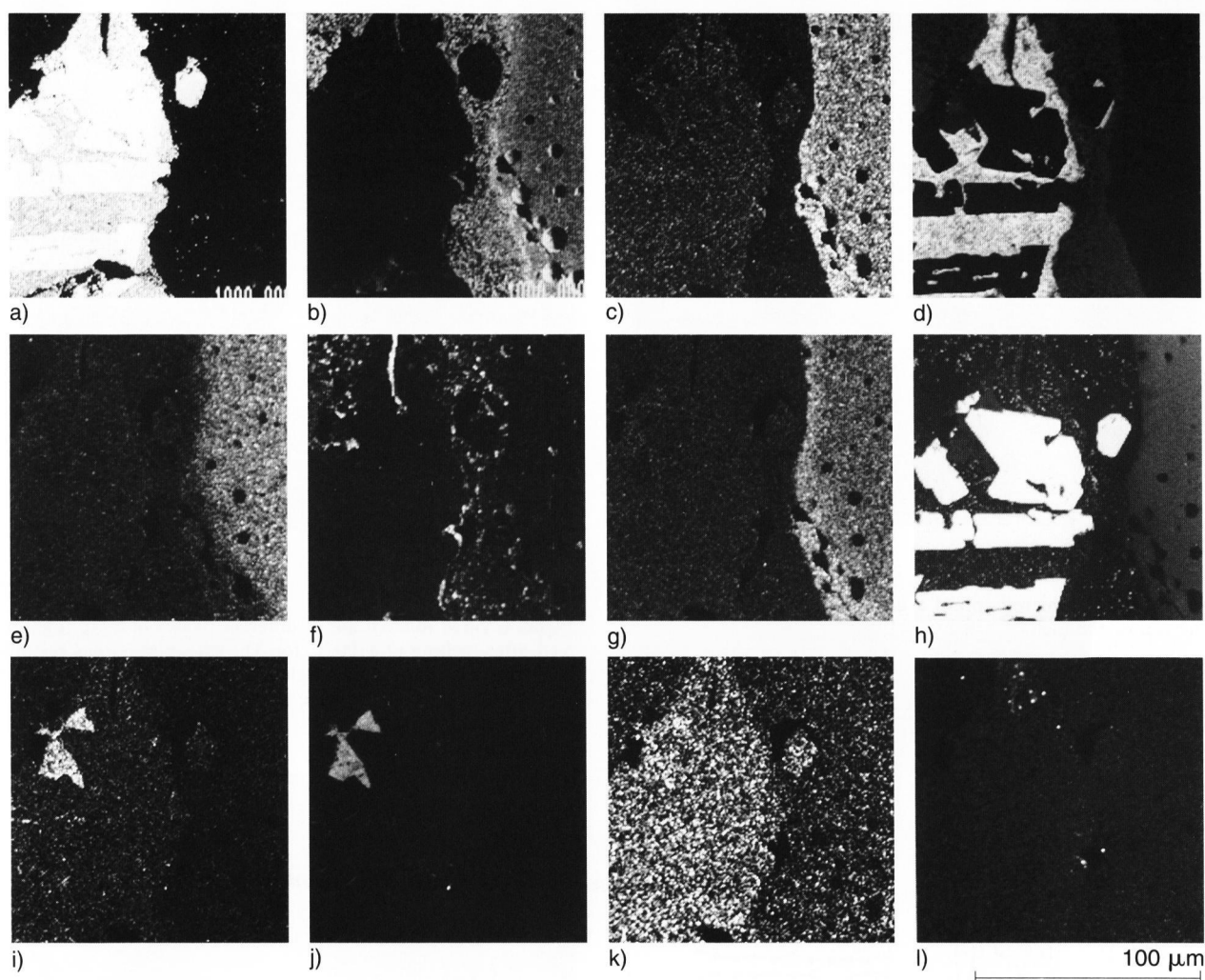
using a SEM DSM 940 A (Carl Zeiss, Oberkochen (Germany)). This was done to clarify the formed phases and the reaction mechanism with the aid of quantitative X-ray microanalyses (EDX analyses).

Figures 3a to l show an X-ray elemental mapping of a gray/black-colored glass region which occurred at the bottom of the crucible. The aluminum introduced (0.1 g) was not dissolved completely after annealing at 1300 °C for 48 h. The gray glass regions possess a higher and very strong fluctuating aluminum content than the bulk glass and are composed of different phases. There was found an aluminum–silicon alloy also containing still other elements such as manganese, iron, nickel, copper, phosphorus which occurred in different distributions and concentrations. The pure silicon is embedded in this alloy.

Between this phase and the surrounding glass a porous region occurs which appears in the micrograph obtained with backscattered electrons (BSE) as a light and a dark phase. These phases are too small to analyze their composition exactly. Since the mainly occurring elements are aluminum, silicon and oxygen, these regions may in principle be composed of aluminum, Al_2O_3 , SiO_2 , silicon or mullite. At the interface gray glass/bulk glass many bubbles are observed. In the top part of crucible melt, the silicon appears in spherical form. It is embedded in the aluminum-rich gray glass phase (figure 4) and not in an aluminum–silicon alloy.

Also line scans of this sample (figure 5) confirmed that element concentrations fluctuate strongly in the gray glass phase and different phases occur. Both, pure silicon and an aluminum–silicon alloy were found.

The samples melted at 1100 °C showed that by addition of aluminum the glass will separate. In the aluminum-rich glass phase, besides silicon, Al_2O_3 , alloys, and mullite, also a calcium silicate phase was observed (figure 6). This phase was only found in the green and amber glass melts. With longer annealing times the quantity of the aluminum–silicon alloy decreases and alumina and silicon are formed.



Figures 3a to l. Results of X-ray elemental mapping of a gray/black-colored glass region. a) BSE, b) OK_{α} , c) NaK_{α} , d) AlK_{α} , e) CaK_{α} , f) PK_{α} , g) KK_{α} , h) SiK_{β} , i) MnK_{α} , j) FeK_{α} , k) NiK_{α} , l) CuK_{α} .

If magnesium is introduced in the melt, silicon spheres with similar composition appear. The glass around the spheres is separated into two phases, a calcium silicate-rich glass phase and a calcium silicate-poor glass phase (figure 7). Figure 8 shows a BSE micrograph of a sample prepared at 1200 °C. The gray glass regions also contain different phases and porous regions. The light phase is magnesium calcium-enriched. The concentration of silicon and oxygen is small and irregularly distributed in this phase. The magnesium is also concentrated in the dark porous regions and occurs as oxide or silicate.

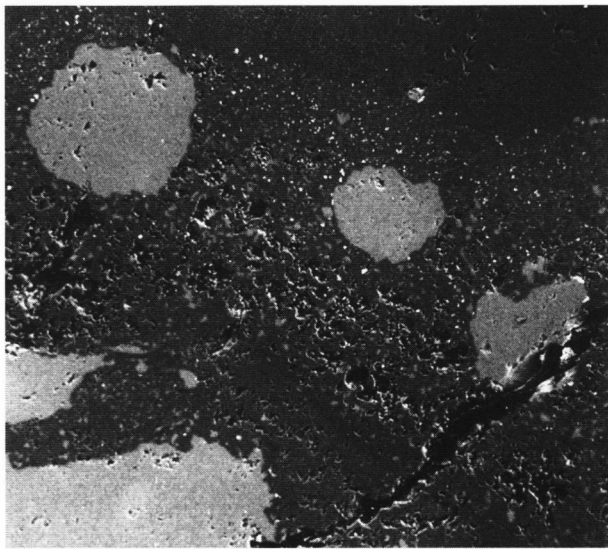
The study confirms that the aluminum will be dissolved in the container glass melt. But the formed silicon remains in the melt and dissolves only after very long annealing times at high temperatures. In contrast to literature [2, 3 and 15], it was found that aluminum causes the formation of silicon spheres in the container glass melt. But other metals such as magnesium can also

induce the formation of metallic inclusions. With the aid of electron microscopy, it was shown that different phases are formed during the melting process.

6. Discussion

Aluminum is stable in the container glass melt up to high temperatures and dissolves with a small reaction rate. The dissolution rate of the metal depends on oxygen partial pressure in the melt, the quantity of aluminum introduced and melting conditions (time, temperature, glass volume).

Melts at different temperatures showed the following phases: at low temperatures an aluminum-rich glass phase with aluminum-silicon alloys, aluminum oxide, mullite, silicon and calcium silicate were found. The formed aluminum alloys, not completely oxidized aluminum and small silicon particles color the glass gray, brownish and black. With increasing aluminum



100 μm

Figure 4. BSE micrograph of a gray-colored glass region from the top of the melt.

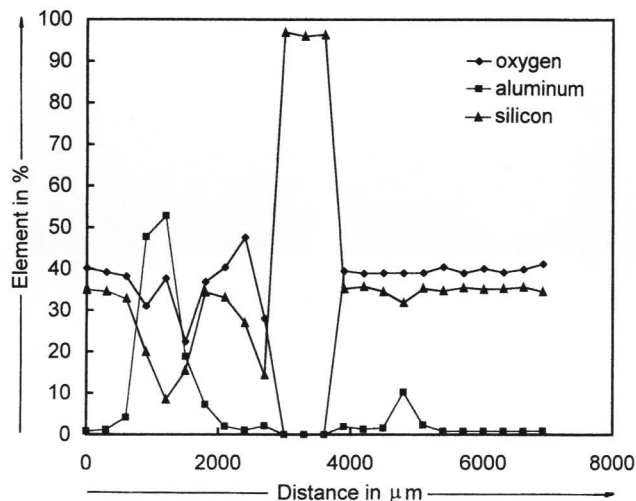
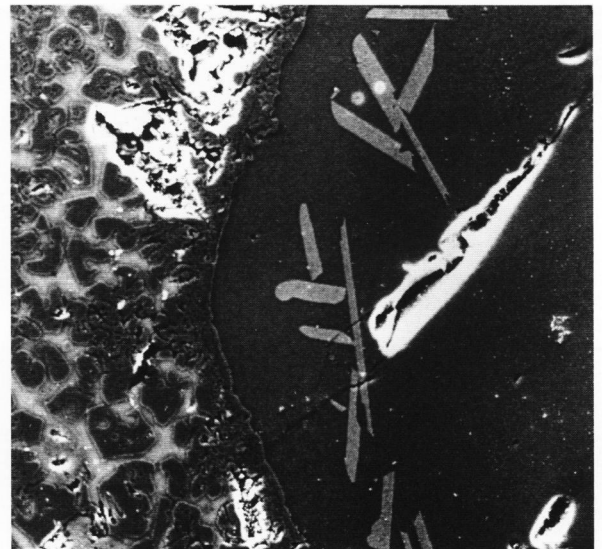


Figure 5. Quantitative line scan of the gray-colored glass region in figure 4.

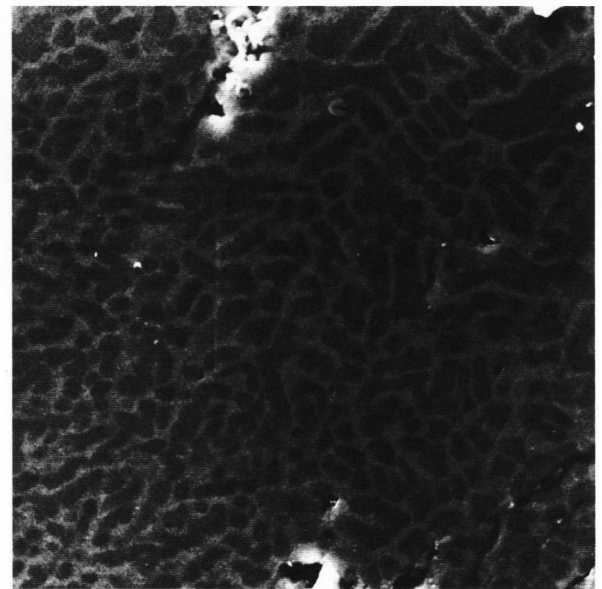
content, the dissolution rate of aluminum decreases. Higher temperatures and longer melting times are necessary to obtain clear glass melts. The aluminum reacts with dissolved oxygen, hydroxide ions, polyvalent ions and silicates in the melt. Figure 9 shows a reaction scheme of oxidation and reduction processes which are assumed to occur. The reactions may run parallel and hence, the reaction mechanism will be complicated.

Thermodynamic calculations using data from [19] confirm that all assumed reactions (figure 10) are possible. With increasing temperature the ΔG_r^0 value of the formation of mullite decreases, while all other ΔG_r^0 values increase. From the introduced aluminum only 2



100 μm

Figure 6. SEM micrograph of different phases in a green glass melt after melting at 1100°C for 3 h; left: gray porous region composed of a dark and a light phase, right: gray glass with lamellae of the calcium silicate phase.



20 μm

Figure 7. SEM micrograph of phase separation of glass after magnesium addition (melted at 1550°C for 4 h),

to 3% reacts to silicon. The main part of metal will be oxidized through dissolved oxygen, hydroxide and polyvalent ions.

In green and amber glass the reaction mechanism is similar to that in flint glass. But fewer silicon spheres and a higher dissolution rate have been observed. These results should mainly be caused by higher surface temperatures and lower viscosity in the amber glass melt [4].

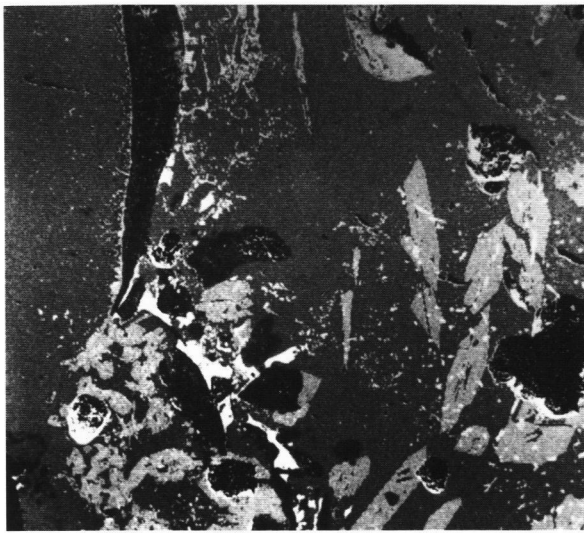


Figure 8. BSE micrograph of a gray glass after addition of magnesium cuttings (melted at 1200 °C).

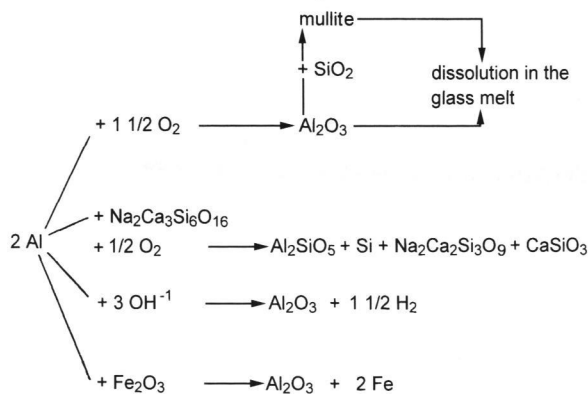


Figure 9. Reaction scheme of oxidation and reduction processes by addition of aluminum.

Caused by the reducing melting conditions, the amber glass possesses a higher content of Fe^{2+} ions, which increases the bath temperature by strong absorption of the heat radiation. Also the formation of mullite confirms the higher temperature at the melt surface. The polyvalent ions in the melt may accelerate the oxidation of metal.

In contrast to aluminum small amounts of magnesium will be dissolved in the container glass melt. The magnesium reacts strongly with calcium compounds. A magnesium–calcium alloy, metal oxide phases and silicates are formed. With increasing magnesium input the melts become also gray, black, brown colored and contain silicon spheres possessing a similar structure. In a further publication, there will be reported on the structure of silicon spheres formed in laboratory melts and during the production process.

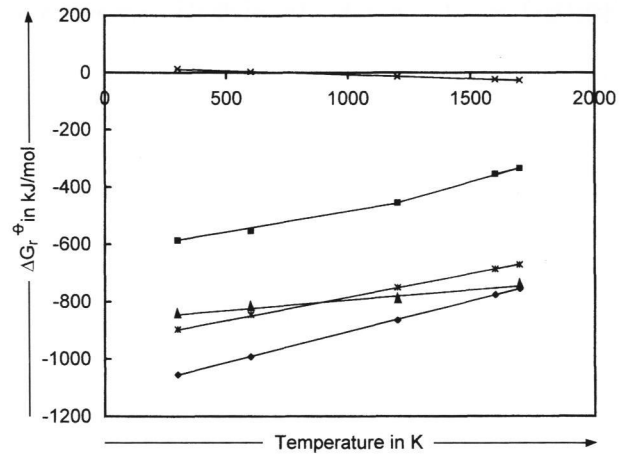
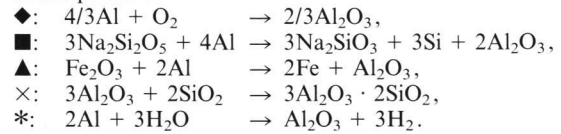


Figure 10. Standard free enthalpy, ΔG_r^0 , calculated as a function of temperature.



7. Conclusions

The dissolution of aluminum in container glass melts is a complicated process which leads to the formation of silicon spheres. Caused by their very small dissolution rate, the silicon spheres are formed in the final glass product and hence, cause production losses. This problem can only be solved by further improvements in the preparation process of cullet. The metallic contaminations must completely be separated.

*

These investigations were conducted with the kind support of the Arbeitsgemeinschaft industrieller Forschungsvereinigungen (AiF), Köln, (AiF-No. 9385B) under the auspices of the Hüttentechnische Vereinigung der Deutschen Glasindustrie (HVG), Frankfurt/M., utilizing resources provided by the Bundesminister für Wirtschaft, Bonn. Thanks are due to all these institutions and to the Oberland Glas AG, Bad Wurzach.

8. References

- [1] Schulte, K.: Voreilende Bodenkorrosion in Glasschmelzöfen durch Metalle. *Glastech. Ber.* **50** (1977) no. 8, p. 181–185.
- [2] Weiser, S.; Leblanc, J.; Kilpatrick, B. et al.: How aluminum metal contamination affects container production. *Glass Ind.* **67** (1986) no. 7, p. 14–19.
- [3] Schumacher, L.: Entstehung von elementarem Silicium in einer Grünglassschmelze bei extrem hohem Scherbenzusatz. Presented at: Meeting of Technical Committee III of DGG on April 9, 1975 in Frankfurt/M.
- [4] Wischnat, V.; Roger, U.; Lenhart, A.: Formation and oxidation of silicon in container glass melts. *Glastech. Ber.* **66** (1993) no. 11, p. 285–289.

- [5] Hard, R.; Maurin, J. K.: The nucleation and growth of oxide islands on aluminum. *Surface Sci.* **20** (1970) p. 285–303.
- [6] Altenpohl, D.: *Aluminium and Aluminiumlegierungen*. Berlin (et al.): Springer, 1965.
- [7] Thiele, W.: Die Oxidation von Aluminium- und Aluminiumlegierungsschmelzen. *Aluminium* **38** (1962) no. 11, p. 707–715; no. 12, p. 780–786.
- [8] Smeltzer, W. W.: Oxidation of an aluminium 3 per cent magnesium alloy in the temperature range 200–500 °C. *J. Electrochem. Soc.* **105** (1958) no. 2, p. 67–71.
- [9] Gmelin: *Handbuch der anorganischen Chemie*. Syst. Nr. 35, T. A. Aluminium. Chemie Berlin: Verl. 1934/35.
- [10] Froberg, M. G.: *Thermodynamik für Metallurgen und Werkstofftechniker*. Leipzig: VEB Deutscher Verl. Grundstoffindustrie 1980.
- [11] Shardakov, N. T.; Karpov, B.; Kudyakov, V. Y. et al.: Products of interaction of glass oxide melts with aluminized steels. *Glass Ceram.* **48** (1991) no. 10, p. 461–464.
- [12] Standage, A. E.; Gani, M. S.: Reaction between vitreous silica and molten aluminum. *J. Am. Ceram. Soc.* **50** (1967) no. 2, p. 101–105.
- [13] Petermöller, H.: Laborversuche zur Bestimmung der Herkunft von Siliciumeinschlüssen im Glas. Presented at: Meeting of Technical Committee III of DGG on April 9, 1975 in Frankfurt/M.
- [14] Lindsay, J. G.; Bakker, W. T.; Dewing, E. W.: Chemical resistance of refractories to Al and Al–Mg alloys. *J. Am. Ceram. Soc.* **47** (1964) no. 2, p. 90–94.
- [15] Wohlleben, K.; Woelk, H.; Konopicky, K.: Untersuchung kugeligter Einschlüsse im Flachglas mit Hilfe der Elektronenstrahlmikroanalyse. *Glastech. Ber.* **39** (1966) no. 7, p. 329–332.
- [16] Petzold, A.; Hinz, W.: *Silikatchemie. Einführung in die Grundlagen*. Leipzig: VEB Deutscher Verl. Grundstoffindustrie 1978.
- [17] *Aluminium-Taschenbuch*. 14. Aufl., 3. Nachdr. Düsseldorf: Aluminiumverl. 1988.
- [18] Bauermeister, F.; Frischat, G. H.; Henicke, H. W.: Auflösungsverhalten tonerdehaltiger Rohstoffe in der Glasschmelze. *Glastech. Ber.* **50** (1977) no. 2, p. 35–44.
- [19] Knacke, O.; Kubaschewski, O.; Hesselmann, K.: *Thermochemical properties of inorganic substances*. 2nd ed. Berlin (et al.): Springer 1991.

■ 0596P002

Address of the authors:

R. Reisch, D. Stachel, S. Traufelder, E. Tessmann
Friedrich-Schiller-Universität, Otto-Schott-Institut,
Fraunhoferstraße 6, D-07743 Jena